Journal of Environmental Chemical Engineering 5 (2017) 2128–2141

Contents lists available at ScienceDirect

Journal of Environmental Chemical Engineering

journal homepage: www.elsevier.com/locate/jece

Novel metal-doped bacteriostatic hybrid clay composites for point-of-use disinfection of water

Emmanuel I. Unuabonah[a,*], Matthew O. Kolawole[b], Foluso O. Agunbiade[a,*], Martins O. Omorogie[a], Daniel T. Koko[a], Chidinma G. Ugwuja[a], Leonard E. Ugege[a], Nicholas E. Oyejide[c], Christina Günter[d], Andreas Taubert[e]

[a] Environmental & Chemical Processes Research Laboratory, Department of Chemical Sciences, Redeemer's University, P.M.B 230, Ede, Osun State, Nigeria
[b] Infectious Diseases and Environmental Health Research Laboratory, Department of Microbiology, University of Ilorin, Ilorin, Kwara State, Nigeria
[c] Department of Biological Sciences, Redeemer's University, P.M.B 230, Ede, Osun State, Nigeria
[d] Department of Earth and Environmental Science, University of Potsdam, D-14476, Potsdam, Germany
[e] Institute of Chemistry, University of Potsdam, D-14476 Potsdam, Germany

ARTICLE INFO

Keywords:
Kaolinite
Composites
Bacteria
Breakthrough time
Regeneration

ABSTRACT

This study reports the facile microwave-assisted thermal preparation of novel metal-doped hybrid clay composite adsorbents consisting of Kaolinite clay, *Carica papaya* seeds and/or plantain peels (*Musa paradisiaca*) and $ZnCl_2$. Fourier Transformed IR spectroscopy, X-ray diffraction, Scanning Electron Microscopy and Brunauer–Emmett–Teller (BET) analysis are employed to characterize these composite adsorbents. The physicochemical analysis of these composites suggests that they act as bacteriostatic rather than bacteriacidal agents. This bacterostactic action is induced by the ZnO phase in the composites whose amount correlates with the efficacy of the composite. The composite prepared with papaya seeds (PS-HYCA) provides the best disinfection efficacy (when compared with composite prepared with *Musa paradisiaca* peels-PP-HYCA) against gram-negative enteric bacteria with a breakthrough time of 400 and 700 min for the removal of 1.5×10^6 cfu/mL *S. typhi* and *V. cholerae* from water respectively. At 10^3 cfu/mL of each bacterium in solution, 2 g of both composite adsorbents kept the levels the bacteria in effluent solutions at zero for up to 24 h. Steam regeneration of 2 g of bacteria-loaded *Carica papaya* prepared composite adsorbent shows a loss of ca. 31% of its capacity even after the 3rd regeneration cycle of 25 h of service time. The composite adsorbent prepared with *Carica papaya* seeds will be useful for developing simple point-of-use water treatment systems for water disinfection application. This composite adsorbent is comparatively of good performance and shows relatively long hydraulic contact times and is expected to minimize energy intensive traditional treatment processes.

1. Introduction

Most current outbreak of diseases in the world is caused by water and foodborne enteric bacteria, such as cholera (caused by *Vibrio cholera*), diarrhoea, dysentery (caused *by Escherichia coli*), food poisoning, typhoid (caused by *Salmonella typhi*). It is reported globally that no fewer than 1.8 billion people utilize a drinking-water source polluted with faeces [1]. Reports from world health organization confirmed that approximately 1.8 million people die annually as a result of diarrheal related diseases [2]. In Nigeria, diarrhoea and other water-borne diseases lead to the death of young children more than Human Immunodeficiency Virus (HIV), malaria and measle combined [3]. About 88% of diarrhoea disease is attributed to unsafe water supply and hygiene [4]. World Health Organization (WHO) reported that *E. coli* contaminated drinking water is estimated to cause 502,000 deaths each year [1]. The source of infection may be attributed to the transportation of pathogens from manure to ground water by leaching and precipitation as observed by Gagliardi et al. [5–8].

Point-of-use (POU) water treatment systems find very strong relevance in areas hit by natural disaster and in several developing countries of the world where municipal water treatment and management is very poor. With POU systems, the need for chemicals and/or energy application is eliminated.

Water disinfection processes include the destruction and removal of microorganisms via a number of techniques such as; physical processes, for example adsorption, distillation and filtration [9]; biological processes [10]; physicochemical processes such as flocculation or lime softening, chlorination and ozonation [11]; electromagnetic radiation

* Corresponding authors.
E-mail addresses: unuabonahe@run.edu.ng, iyaemma@yahoo.com (E.I. Unuabonah), foagunbiade@gmail.com (F.O. Agunbiade).

http://dx.doi.org/10.1016/j.jece.2017.04.017
Received 20 December 2016; Received in revised form 7 April 2017; Accepted 8 April 2017
Available online 10 April 2017
2213-3437/

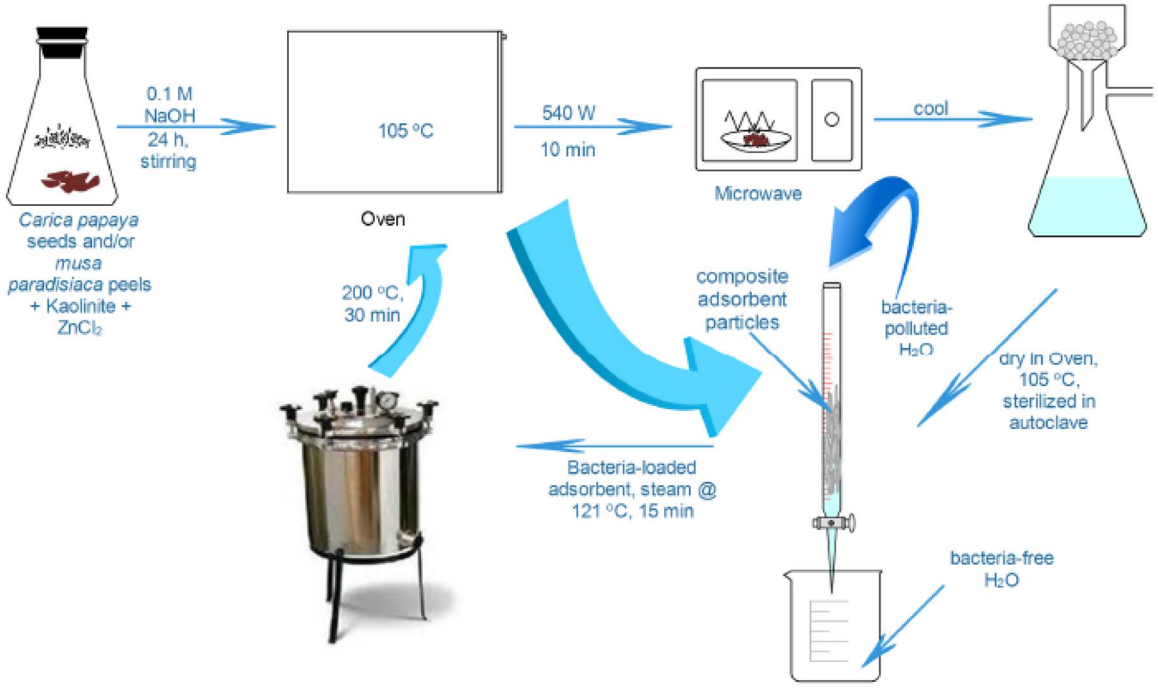

Scheme 1. Preparation of Zn-doped Hybrid Clay bacteriostatic composites for removal of enteric bacterial from water.

[12] and photocatalytic processes [13].

Chemical agents (such as chlorine and its compounds) are most widely used because of their effectiveness, low cost [14] and their extra protection against regrowth of bacteria and pathogens [15] which give it an advantage over other purifying processes. However, the addition of these chemicals to water can alter the taste of the water and also react with various constituents in natural water such as Dissolved Organic Matter (DOM) to form disinfection by-products, many of which are carcinogens [16]. Also, some microorganisms are resistant to chemical disinfectants, in this case, high dosage of the chemical disinfectant will be required leading to the formation of a significant amount of disinfectant by-products [17].

Recently, adsorption technique has been a favoured method to remove bacteria and viruses in water because it is simple, offers high efficiency, relatively cheap to operate, and the availability of raw materials [18]. Furthermore, adsorption processes do not produce by-products unlike chemical disinfection processes such as chlorination. Several adsorbents have been evaluated for the process of adsorption, some of which include both conventional and non-conventional materials [19] but over time nanoparticles have found wide acceptance for the removal of bacteria from water [20–22]. However, there are now growing concerns about their toxicity both to man and the environment, especially with silver-mediated nanoparticles [20,23,24]. Beyond their toxicity, there are the issues of aggregation in water (due to their very small sizes) and the complexity involved in post-treatment procedures. This has led to a growing need for materials with excellent treatment capacities, which are non-toxic, cheap and readily available.

In considering water disinfection, the performance and cost of the disinfectant are important factors to consider. Current technologies utilizing membrane or silica-based materials are very expensive though very efficient. Cheap and yet highly efficient functional materials that can be used for the disinfection of very large volumes of water are, therefore, highly sought after [25].

To reduce cost while retaining the efficacy of the material, and to overcome the shortcomings of metal-mediated nanoparticles, naturally available materials like kaolinite, *Carica papaya* seeds and *Musa paradisiaca* peels (plantain peels) would provide a sustainable source of raw materials for the development of bacteriostatic composites. We have previously described the synthesis and performance of a new composite material based on a composite of kaolinite and *Carica papaya* seeds for water treatment [26]. However, this composite material failed as a bactericidal or bacteriostatic agent. Its low-cost, and excellent water permeability (flowrate) under gravity has inspired the engineering of this material to suit the purpose of disinfection of water. In this study, bacteriostatic composites are developed from a combination of kaolinite, *Carica papaya* and/or plantain peels and $ZnCl_2$ under a microwave-assisted thermal process.

An advantage of the composite development process in this study is that no high pressure or additional (expensive) organic template is required; the microwave irradiation utilizes low energy, is rapid and leads to shorter pyrolysis time. The resulting composites show high efficiencies for the removal of *Vibrio Cholerae* and *Salmonella typhi* in water. Zinc is biocidal yet it is found in cells throughout the body. It is needed for the body's defensive (immune) system to properly work. It plays a role in cell division, cell growth, wound healing, and the breakdown of carbohydrates. Zinc is also needed for the senses of smell and taste. Zinc was doped into the composite materials utilized in this study to improve their antibacterial properties.

2. Materials and methods

2.1. Materials

Raw Kaolinite clay was obtained from Redemption City, Mowe, Ogun State, Nigeria. After collection, stones, and other dense particles were removed from the sample. The sample was purified according to reported protocols [27]. *Carica papaya* seeds and plantain peels (*Musa paradisiaca*) were sourced from several open markets in Nigeria and sun-dried. The dried *papaya* seeds and plantain peels were then crushed and collected into an air-tight container. Zinc chloride anhydrous pellets > 97% purity (Sigma-Aldrich), Sodium hydroxide pellets (NaOH), Hydrogen peroxide (H_2O_2), Sodium chloride (NaCl), Nutrient agar (HiMedia Laboratories Pvt. Ltd India), Nutrient broth (Rapids labs Little Bentley, Colchester UK), Thiosulfate-Citrate-Bile-Sucrose (TCBS) Agar (Rapids Labs, Little Bentley, Colchester, UK), *Salmonella-shigella* (SS) Agar (HiMedia Laboratories Pvt. Ltd) were used as purchased. The

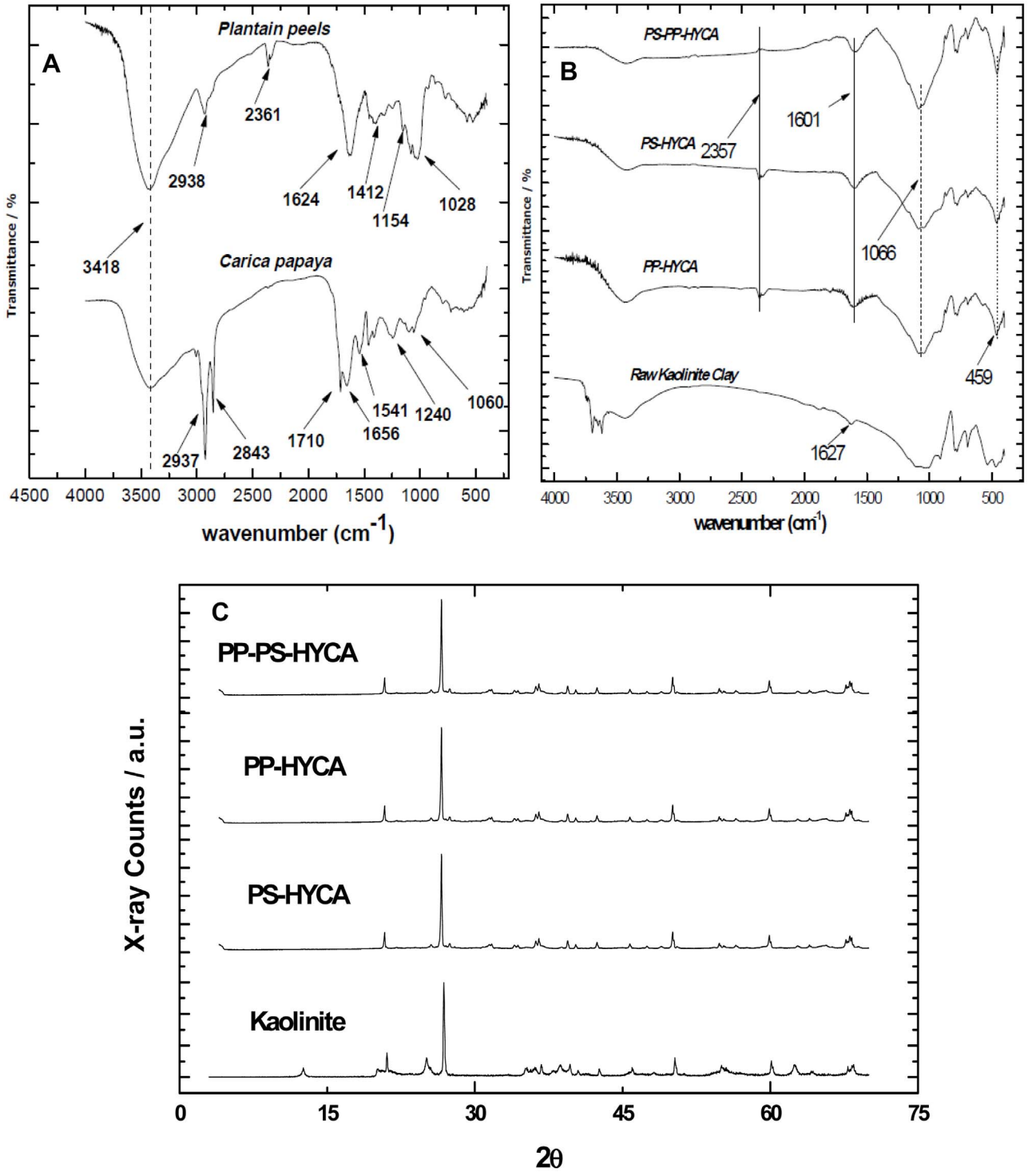

Fig. 1. Fourier Transformed Infrared Spectra of (A) *Carica papaya* seeds and *Musa paradisiaca* (Plantain peels) (B) kaolinite, *Carica papaya*-kaolinite (PS-HYCA) and plantain peel-kaolinite (PP-HYCA), *Carica papaya*-plantain peel-kaolinite (PS-PP-HYCA) composite adsorbents. (C) X-ray Diffraction pattern for Kaolinite, PS-HYCA, PP-HYCA and PS-PP-HYCA composite adsorbents.

pure culture of the test bacteria employed in this study: *V. cholerae* (ATCC 25837) and *S. typhi* (ATCC 13311), were obtained from the Department of Biological Sciences, Redeemer's University, Nigeria. They were used as obtained.

2.2. Metal-doped hybrid clay synthesis

The schematic diagram for the preparation regeneration and reuse of metal-doped hybrid clay composites is shown in Scheme 1. An amount of $ZnCl_2$ (3.0 g) was weighed into a 100 mL beaker with 2.0 g each of purified kaolinite clay and crushed *Carica papaya* seeds. The mixture was dispersed in a 10 mL solution of 0.1 M NaOH and stirred continuously for 24 h to allow for impregnation of Zn into the mixture. It was then transferred to the oven at 105 °C to dry. The oven dried mixture was then transferred into a microwave system and was calcined at 540 W for 10 min. The prepared material was then removed and washed with distilled water using a 0.45 μm filter paper in a vacuum filtration system to a neutral pH of 7.0. The synthesized material was

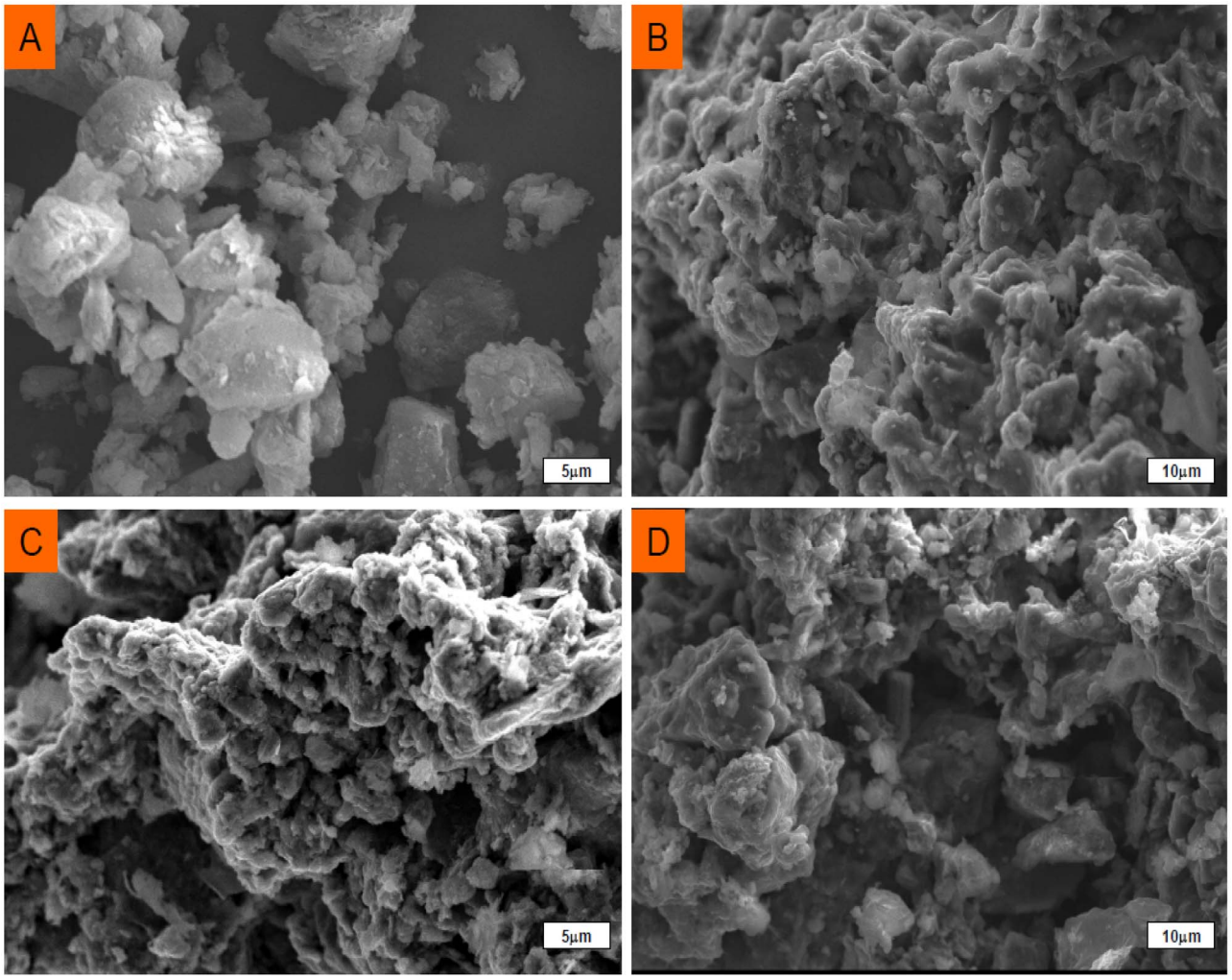

Fig. 2. Scanning Electron Microscopy Images of (A) Kaolinite (B) PP-HYCA = plantain peel-Hybrid clay composite adsorbent; (C) PS-HYCA = *Carica papaya* seeds-Hybrid Clay composite adsorbent (D) PS-PP-HYCA = Papaya seeds-Plantain peel-Hybrid Clay composite adsorbent (Plantain Peel = *Musa* spp.).

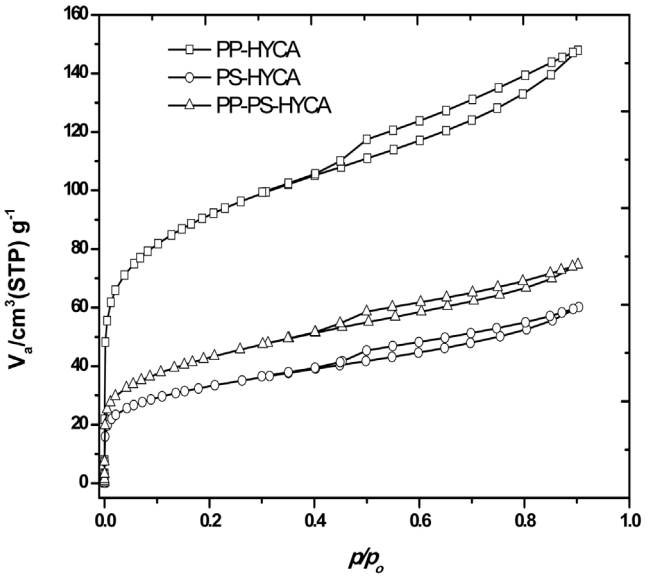

Fig. 3. N_2 adsorption/desorption isotherms (77.4 K) for composite adsorbents prepared via microwave @ 540 W for 10 min.

dried in an oven at 105 °C to constant weight, packed in an airtight container and labelled as PS-HYCA. Similarly, the plantain peels-clay composite adsorbent (PP-HYCA) was prepared by mixing 3.0 g of $ZnCl_2$ with 2.0 g each of purified kaolinite clay and grinded *Musa paradisiaca* peels in a 100 mL beaker containing 10 mL of 0.1 M sodium hydroxide. This mixture was stirred continuously for 24 h and subsequently transferred to an oven to dry at 105 °C. The oven dried mixture was then transferred to the microwave equipment and was calcined at 540 W for 10 min. The *Carica papaya*-plantain peel-clay composite adsorbent (PS-PP-HYCA) was prepared by mixing 3.0 g of $ZnCl_2$ with 2.0 g of purified kaolinite clay and 1.0 g each of ground *Carica papaya* seeds and plantain peels in a 100 mL beaker containing 10 mL of 0.1 M NaOH. This mixture was stirred continuously for 24 h and subsequently transferred to an oven to dry at 105 °C. The oven dried mixture was then transferred to the microwave equipment and was calcined at 540 W for 10 min.

2.3. Characterization of materials

2.3.1. X-ray diffraction (XRD)

X-ray diffraction (XRD) patterns were recorded on a Siemens D-5000 x-ray powder diffraction system (Cu-anode X-ray tube) with 20 mg of well-ground clay sample placed in a 20-mm square hole in the center of a 2-mm thick sample holder. XRD patterns were collected with Cu Kα (0.15418 nm) radiation in a Siemens D5000 diffractometer at 40 kV and 30 mA in an angular range of 3–70° 2θ. Counts were

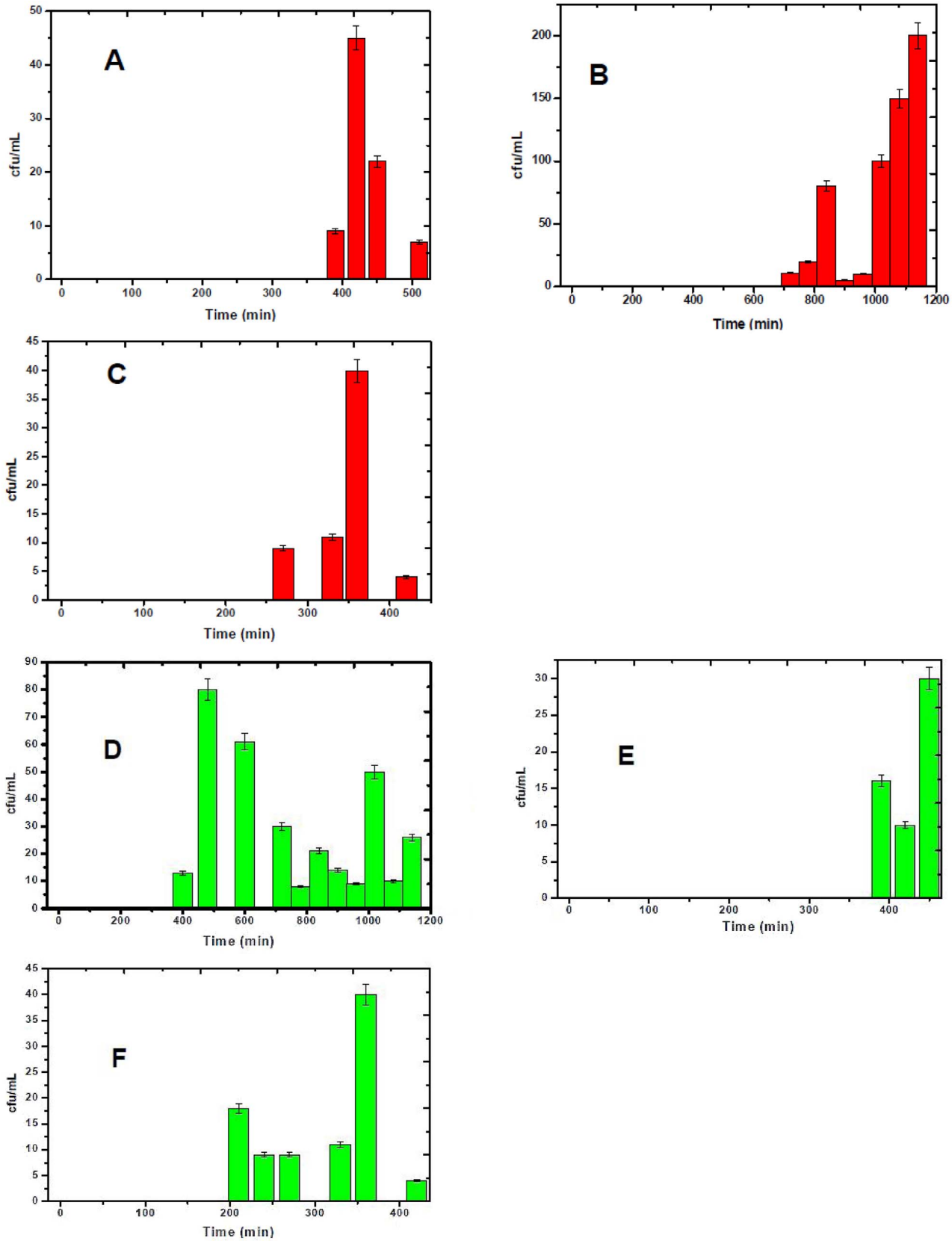

Fig. 4. Breakthrough plots for the removal of ***S. typhi*** from (A) PP-HYCA (B) PS-HYCA (C) PP-PS-HYCA composite adsorbents; ***V. cholerae*** (D) PP-HYCA (E) PS-HYCA (F) PP-PS-HYCA composite adsorbents.

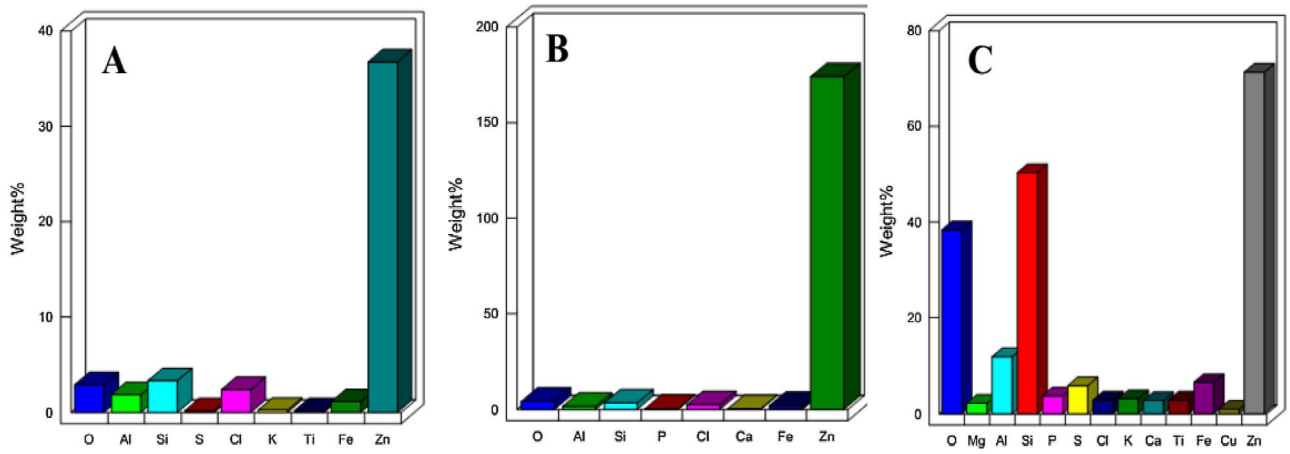

Fig. 5. Scanning Electron Microscopy Micro Elemental analysis of (A) PP-HYCA, (B) PS-HYCA and (C) PP-PS-HYCA composite adsorbents.

recorded with a step size of 0.02° (2θ) and a counting time of 4 s step^{-1}.

2.3.2. Scanning electron microscopy (SEM)

Scanning electron microscopy (SEM) was done on a JEOL JSM 6510 SEM equipped with an EDX spectrometer of Oxford (INCA x-ACT EDS detector). For Energy Dispersive X-ray Analysis (EDX), samples were coated with carbon of thickness of 15 nm. The Back Scattered Electron (BSE) Detector was used for material contrast images at 20 kV. The Secondary Electron (SE) detector was used for topographic imaging at 7 kV.

2.3.3. The point of zero charge (PZC)

The pH of the point of zero charge (pH_{PZC}) was determined by using the salt addition method [28]. 0.03 g of the adsorbent materials was added to 10 mL of 0.01 M NaCl solution with pH ranging of 2.0-12.0 for 24 h. After 24 h the final pH of the solution was recorded and subtracted from the initial pH values. The change in pH was plotted against the initial pH. The pH at which the change in pH is equal to zero was noted as the pH point of zero charge.

2.3.4. Surface area

Surface area determination was done on an AS1 MP and a Quadrasorb machine (both of Quantachrome Instruments, Boynton Beach/FL, USA). The samples were degassed under high vacuum at 150 °C for 20 h before analysis. Surface areas were calculated by the multipoint Brunauer–Emmett–Teller (BET) model [29]. Pore size distributions were calculated using the QSDFT methodology (part of the QuadraWin 5.05 Software package of Quantachrome Instruments). The QSDFT analysis was obtained from the adsorption branch of the isotherms assuming slit-like micropores and cylindrical mesopores.

2.3.5. Fourier transform infrared spectra

Fourier transform infrared spectra were obtained from transmission measurements (Shimadzu 8400S FT-IR, 4000–400 cm^{-1}, 40 Scans) using KBr pellets prepared with a Shimadzu MHP-1 mini hand press. The grinded KBr powder was pressed with SHIMADZU MHP-1 mini

hand press to form homogenized pellet for background measurement. A 10% dilution of composite samples with KBr (10% sample in 90% KBr) was ground with agate mortar to have a homogenized mixture. A pellet was produced using the SHIMADZUMHP-1 mini hand press. The pellets were placed in sample handle and measurement was taken in the percent transmittance mode. SHIMADZU 8400S FT-IR instrument in the vibrational absorption range of 4000–450 cm^{-1} was employed.

2.3.6. Flame atomic absorption spectroscopy (FAAS)

Flame Atomic Absorption Spectroscopy (FAAS) for the analysis of Zn and Na in water effluent samples was performed on a Perkin-Elmer Analyst 800 high performance FAAS at wavelengths of 213.9 and 589.6 nm respectively using air/acetylene gas. Limit of Detections were at 0.001 mg/L for Zn and 0.008 mg/L for Na.

2.4. Pathogenic pollutant removal

To evaluate the efficiency of the composites for gram-negative bacteria removal from water, commercial Eva® drinking water produced by *Coca-Cola* was used as a standard. The water was initially cultured to investigate the presence of *E. coli, V. Cholerae, and S. typhi respectively* and the absence of these bacteria in the bottled water informed its use as a standard. The pure cultures of a standard strain of *V. cholerae* (ATCC 25837) and *S. typhi* (ATCC 13311) were grown in nutrient broth at 37 °C for 24 h to yield a cell count of 10^8 cfu/mL. Quantification was carried out using the optical method with the use of a UV/VIS spectrophotometer at a wavelength of 600 nm and absorbance recorded. Absorbance value was converted to concentration to obtain the amount bacteria colony forming unit (cfu) per millilitre of the solution using the formula in http://www.genomics.agilent.com/biocalculators/calcODBacterial.jsp?_requestid=56013 to give 10^8 cfu/mL. Cultured bacteria strians were then added to a 1.5 L Eva® water to prepare the desired concentration of the bacteria solution and the remaining pure bacteria culture was preserved in the refrigerator at 4 °C for further use.

A fixed weight (2 g) of an initially sterilized Zn-doped composite material (2 g of composite material dispersed in 70% ethanol and dried to constant weight at 105 °C) was added to a 400 mm × 10 mm column earlier sterilized in an autoclave at 121 °C for 2 h. The column was subsequently flushed with 20 mL of sterile water which was allowed to run out entirely. Simulated contaminated water with a concentration of 1.5×10^6 cfu/mL of the test gram-negative bacteria was allowed through the column containing the composite adsorbent at a flow rate of 8 mL/min. Effluents from the column were collected at specific time intervals and analyzed for the presence of gram-negative bacteria using the pour plate method. One millilitre (1 mL) from each of the test microorganisms samples was spread onto selective agar in plates (Salmonella-shigella agar for *S. typhi and* thiosulphate citrate bile sucrose agar for *V. cholerae*). The plates were then incubated at 37 °C for 24 h, and the number of bacteria colonies developed was counted using a manual bacteria counter. The Colony Forming Unit (CFU) per ml was calculated for each sample at different time intervals by using the following formula:

cfu/mL = No. of colonies × Dilution factor/volume inoculated

Where dilution factor is the reciprocal of the dilution in which the plate count was taken, and Volume inoculated is 0.5 mL.

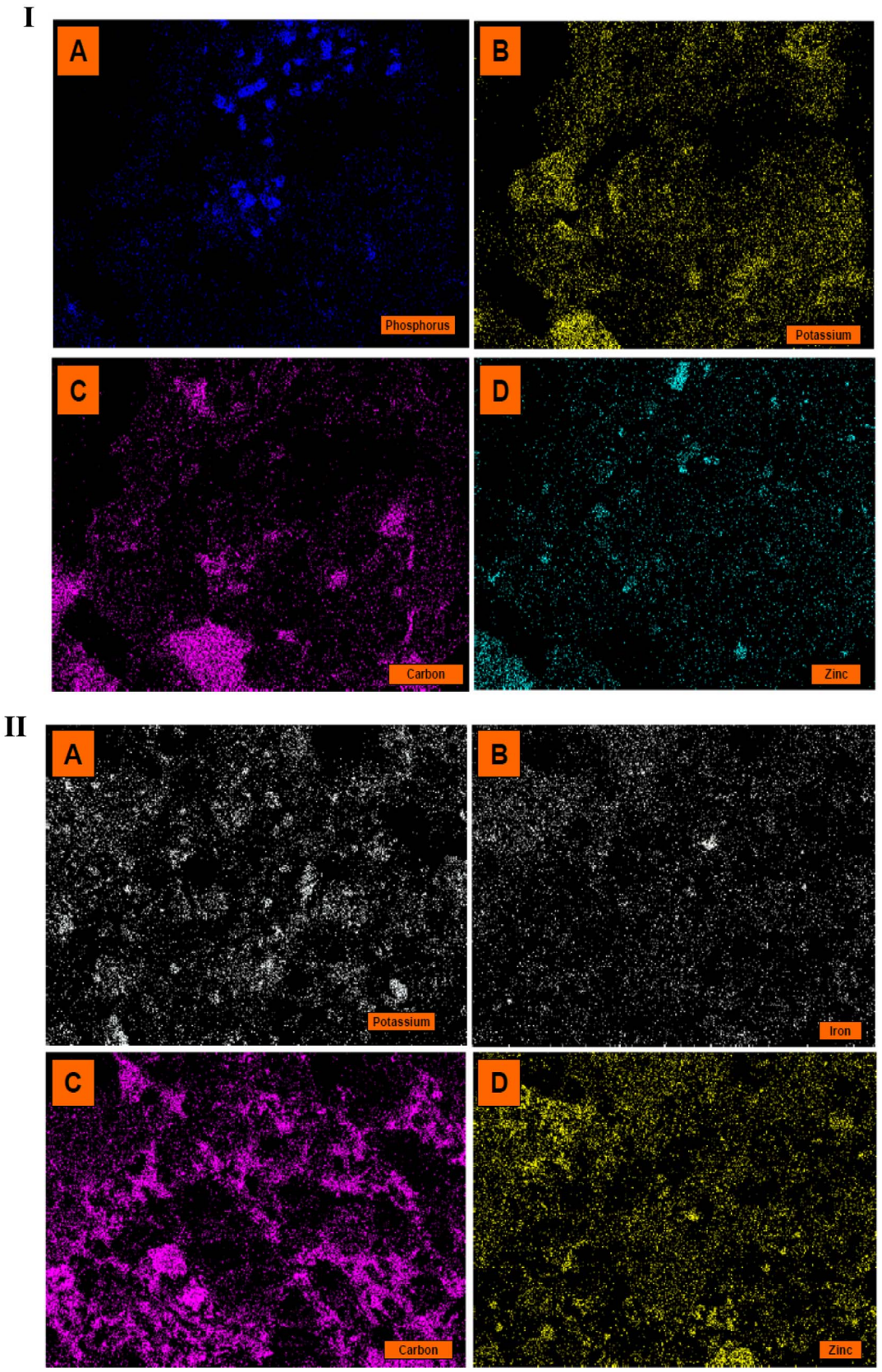

Fig. 6. I. Elemental mapping images of *S. typhi*-loaded PS-HYCA showing the presence and distribution of some of the elemental components of the loaded composite adsorbent. II. Elemental mapping images of *S. typhi*-loaded PP-HYCA composite showing the presence and distribution of some of the elemental components in the bacteria-loaded composite adsorbent.

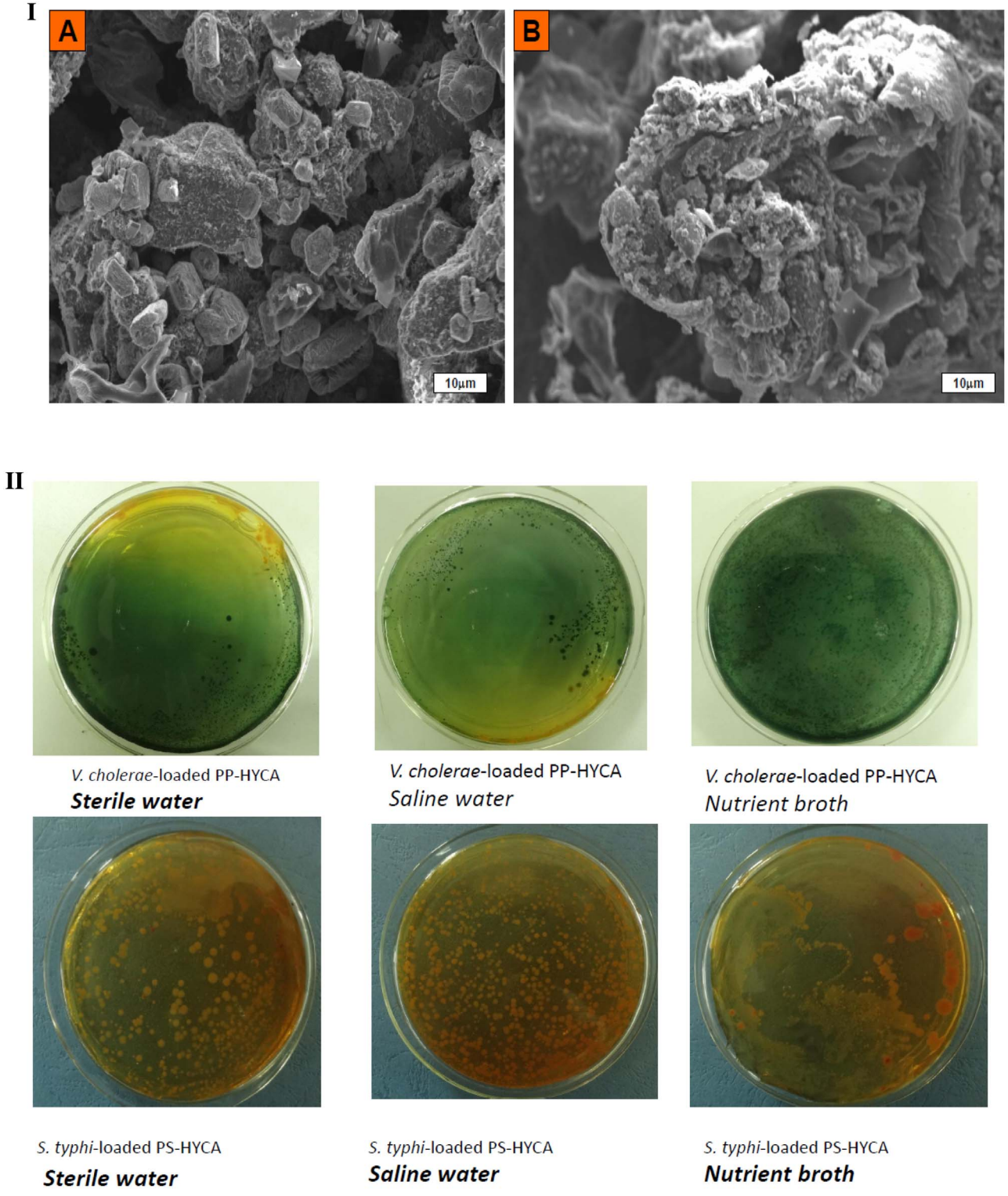

Fig. 7. I. Scanning Electron Microscopy Images of *S. typhi*-loaded (A) PS-HYCA and (B) PP-HYCA composite adsorbents. II. Plates showing the colonies of *V. cholera*e and *S. typhi* desorbed from the surfaces of PP-HYCA and PS-HYCA composite adsorbents using sterile water, saline water and nutrient broth.

A yellowish-orange colour was used to identify *S. typhi* colonies and a green colour was used to identify *V. cholerae* colonies. The break-through point for the column studies was determined as the time for the onset of microbial growth for the test microorganisms.

2.5. Bacteria viability test

Viability test was carried out on bacterial-loaded adsorbents to investigate the mechanism of removal of these gram-negative bacteria from aqueous solutions by PS-HYCA, PP-HYCA and PS-PP-HYCA composite adsorbents. Viability test for bacteria is known to be done by the use of Live/Dead® BacLight™ test kits. However, in this study, we propose a simple method in which three different solutions including normal saline water (0.9% NaCl), sterile water and nutrient broth are used with a vortex mixer. It is thought that the normal saline water would maintain the physiological fluid balance in the bacteria detached

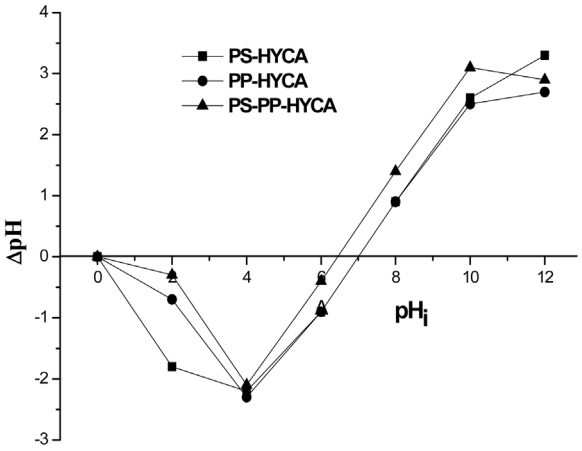

Fig. 8. pH_{pzc} of PP-HYCA, PS-HYCA and PS-PP-HYCA composite adsorbents.

from the particles while the nutrient broth is meant to enrich any 'injured' bacteria present on the surface of the composite adsorbents and help their proliferation.

All three solutions used were sterilized in an autoclave at 121 °C while test-tubes and spatulas were sterilized accordingly. Small quantities of bacteria-loaded composite adsorbents were placed in a test-tube with either 5 mL of saline water, sterile water or nutrient broth. Each solution was vortexed at 2500 rpm for 1 min and allowed to stand for another 1 min. The supernatants were collected afterwards and cultured in the selective agar to determine the viable bacteria in the solution.

2.6. Regeneration

Gram-negative enteric bacteria spent adsorbent was regenerated using Autoclave heating equipment. The exhausted or spent adsorbent was wrapped in aluminum foil and placed inside an autoclave machine for 15 min at 121 °C, after which the adsorbent was dried in an oven at 105 °C and ready for reuse according the method described in Section 2.4.

3. Results and discussions

3.1. Physicochemical analysis

3.1.1. Fourier transform infrared spectroscopy and X-ray diffraction

3.1.1.1. Plantain peel and carica papaya. Fig. 1A represents the Fourier Transformed Infrared (FTIR) spectra for plantain peel and *Carica papaya* seeds. The broad band at 3418 cm^{-1} for both biomasses suggest the presence of an −O−H/−N−H overlap stretching vibration while the peak at ~2937 and 2843 cm^{-1} indicates the presence of an C−H stretch of methyl and methylene [30]. The peak at ~2361 cm^{-1} in plantain peel shows the presence of −C−O bonds. There is a −C═O stretch at 1710 cm^{-1} in the *Carica papaya* seeds which is absent in plantain peel. The very strong peaks at 1624 cm^{-1} for plantain peel and 1656 cm^{-1} for *Carica papaya* seeds are the β- and α-sheets of amide band I of the protein [31].

The region from 1500 cm^{-1} shows peaks for amide band II of protein for both biomasses. The FTIR results indicate that both biomasses contain protein and carbohydrate as well as some amount of cellulose.

3.1.1.2. Composite adsorbents. Fig. 1B illustrates the FTIR spectra of raw kaolinite clay (K), *Carica papaya* seeds-kaolinite (PS-HYCA), plantain peel-kaolinite (PP-HYCA) and *Carica papaya*-plantain peel-kaolinite (PP-PS-HYCA) composites. The kaolinite clay spectrum shows the presence of sharp peaks at 3701 and 3613 cm^{-1} antisymmetric and inner surface −O−H [26,32,33]. The broad band at 3430 cm^{-1} and 1627 cm^{-1} indicate the −O−H is stretching and bending vibrations respectively while the bond at 1065 cm^{-1} indicates the presence of Si-O in-plane bending vibration [34]. The peak at 914 cm^{-1} suggests the presence of Al−O bending in kaolinite whereas peaks appearing at 782 and 684 cm^{-1} indicate the availability of Al−OH bond vibrations [26,35].

The FTIR spectra of composite materials show a disappearance of the peaks at 3701 and 3613 cm^{-1} found in raw kaolinite probably due to heating from the microwave. The spectra of all the composite materials exhibit a strong band at 3418 cm^{-1} suggesting the presence of a combination of −N−H/−O−H stretching vibrations [26]. However, there is the existence of a new absorption band at ~2362 cm^{-1} which is indicative of −C−O stretching vibrations [36] which is weak and inverted in the PS-PP-HYCA composite adsorbent (Fig. 1B). A new peak is observed at 1601 cm^{-1} which suggests the presence of O−H bending vibration [37] in the composite adsorbents (Fig. 1B). There is some change in the shape of the peak at 1065 cm^{-1} for kaolinite when compared with that of the composite adsorbents which could indicate the conversion of Si-O to −Si−O−M [38] where M could be regarded as the Zn used in the activation of the composite formation process. The peak at 459 cm^{-1} implies the presence of ZnO in the composite materials [39,40]. The FTIR spectra, therefore, suggest that a new material (PS-HYCA composite adsorbent) was successfully formed from the combination of kaolinite clay, *Carica papaya* seeds and/or plantain peels and $ZnCl_2$.

To further confirm that a new material has been formed which is different from kaolinite, the composite adsorbents were subjected to X-ray diffraction (XRD). Fig. 1C shows the X-diffraction patterns of the composite materials and kaolinite. Characteristic kaolinite peaks appeared at 12.63° (001), 25.14° (002), 35.26° (131), 36.06° (112), 38.82°(131), 45.92° (203) and 55.02° (204), 60.15° (313) and 62.51° (060) [33,41,42].

However, for the composite materials, peaks at 31.72° (100), 34.21° (002), 46 (101), 56.73° (110), 56 (102), and 62.51° (103) are assigned to Zincite [ZnO, JCPDS 36-1451; [43,44] which supports our earlier report of the presence of ZnO in the composites via FTIR analysis. The peaks at 21.06° and 50.26° are consistent with the presence quartz in the composites [26,45] in the various composite materials with 26.85° being a phase of Quartz [45]. The peaks at 35.90°, 40.7° and 43.65° (Fig. 2) imply that the composites have wurtzite mineral phase which is a hexagonal crystal structure of ZnO [46,47]. The disappearance of the 12.63°and 25.14° peaks with the appearance of a new peak at ca 20.1° in the composites could signify the presence of VPI-8 phase (a Zincosilicate phase) in the composites [48,49].

All of these indicate a change in the crystalline structure of the raw kaolinite used in the preparation of these composites. The ZnO phase found in the composite is a result of the reaction between NaOH and $ZnCl_2$ in the reacting system as shown in the equation below.

$$ZnCl_2 + 2NaOH \rightarrow ZnO + 2NaCl + H_2O \quad (1)$$

The formation of ZnO from reaction between NaOH and $ZnCl_2$ is well established [50].

3.1.2. Scanning electron microscopy (SEM)

The surface morphology of the prepared materials was determined using scanning electron microscope. The SEM images of PP-HYCA, PS-HYCA, and PP-PS-HYCA composites and raw kaolinite clay are shown in Fig. 2. The flaky nature of Kaolinite clay is observed to have changed significantly in the composite adsorbents due to the chemical and thermal treatment during the preparation of the composite adsorbents. From the images, it can be deduced that the prepared adsorbents are composites with average particle size of 0.5 μm. The particles of the composite are smaller in size with no particular shape.

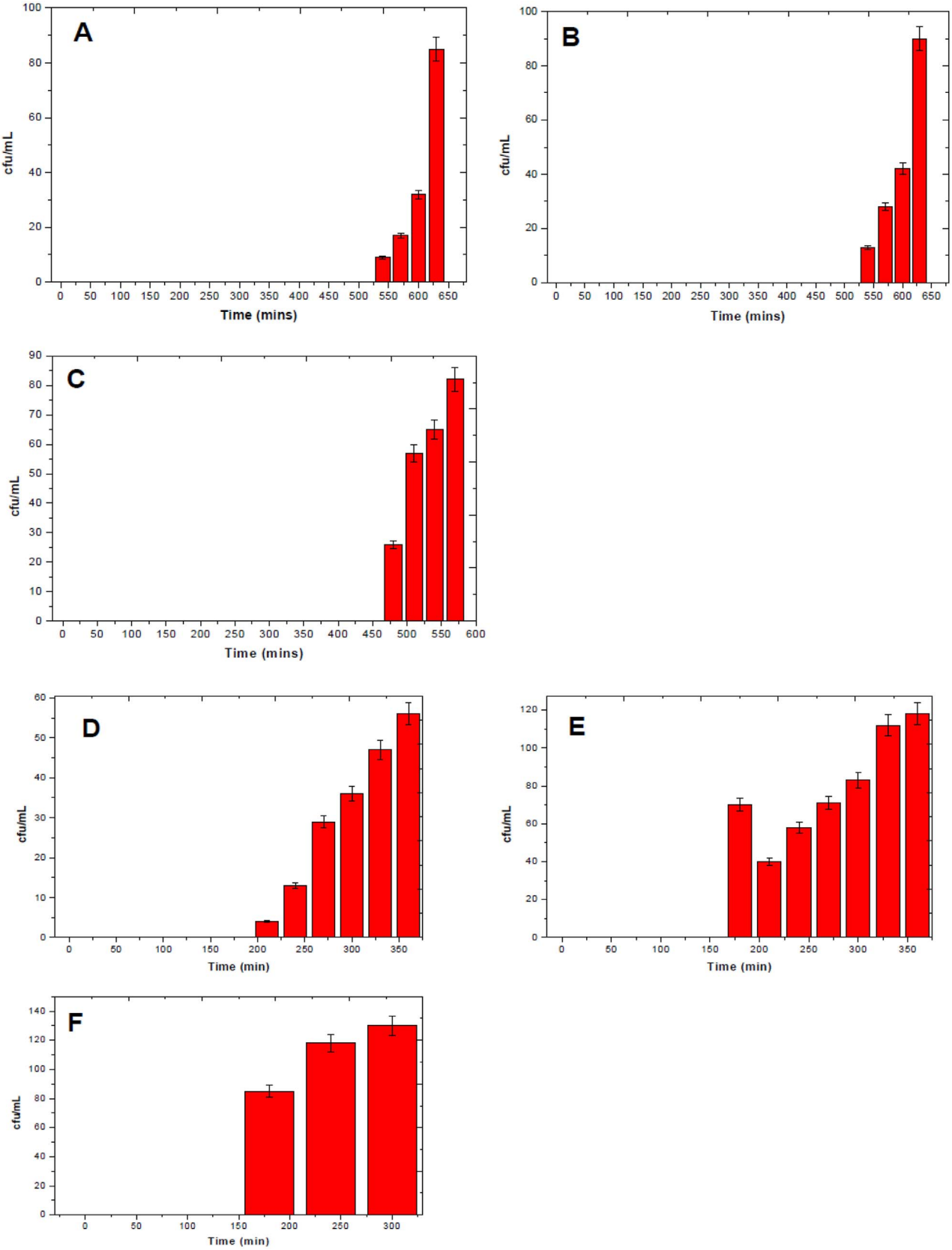

Fig. 9. Breakthrough plots of the performance of steam-regenerated *S. typhi*-loaded *Carica papaya* seed modified kaolinite clay composite adsorbent (PS-HYCA) (A) 1st regeneration cycle (B) 2nd regeneration cycle and (C) 3rd regeneration cycle; steam-regenerated *S. typhi*-loaded plantain peel modified kaolinite clay composite adsorbent (PP-HYCA) (D) 1st regeneration cycle (E) 2nd regeneration cycle and (F) 3rd regeneration cycle.

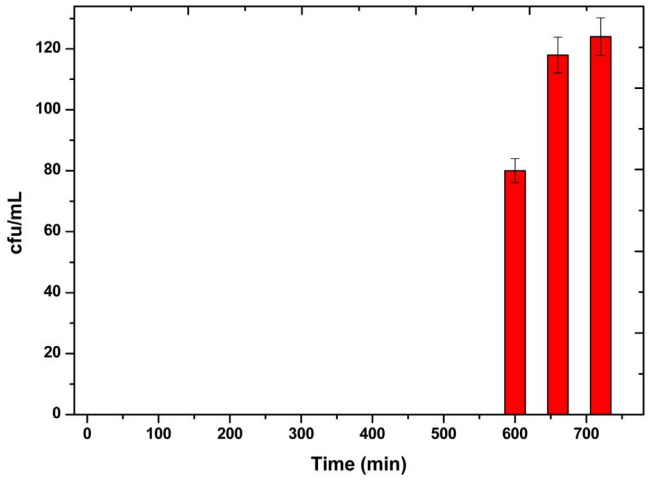

Fig. 10. Performance of Steam-regenerated PS-HYCA composite adsorbent in the removal of *S. typhi* gram-negative bacteria from water.

3.1.2.1. Electron density mapping and microanalysis. The electron mapping analysis of the composite adsorbents is shown in Figs. S1–S3. The electron map image for PP-HYCA composite adsorbent indicates the presence of Fe, K, Cl, and Zn. While that of PS-HYCA composite shows the presence of S, Cl, K, Ca, Fe and Zn. The analysis of PS-PP-HYCA composite signifies the presence of Mg, P, K, Ca, Fe and Zn. All three composites also show the existence of O, Si and Al in them which are essential components of clay (result not shown).

The source of Zn and Cl is the $ZnCl_2$ used as the activating agent for the preparation of the composites; Fe and K constitute part of the chemical composition of plantain peels [51]; Mg and P found in the PS-PP-HYCA composite are from *Carica papaya* seeds and plantain peels [52–54]. It is observed that Zn is uniformly distributed on the surface of PS-HYCA and PP-HYCA composites (Figs. S1 and S2) but is concentrated only at few spots on PS-PP-HYCA composite surface (Fig. S3). Results from microanalysis suggest that the presence of Zn in all composite materials is significant (Fig. S4–S6) and is a prominent component within the composites.

3.1.3. Surface area analysis

Fig. 3 shows the nitrogen adsorption/desorption isotherms of the composite materials. Results show the surface area of PP-HYCA, PS-HYCA and PP-PS–HYCA composite adsorbents to be 324, 117 and 150 m^2/g respectively, while their pore sizes were 2.82, 3.20 and 3.07 nm respectively. The surface areas of these composites are more than 10 times that of kaolinite which was previously measured to be $\approx 9\ m^2/g$ [26].

3.2. Bacterial removal activity

The antibacterial activity of the prepared composites, PS-HYCA, PP-HYCA and PS-PP-HYCA composite adsorbents were tested on gram-negative enteric bacteria, *Salmonella typhimurium* (ATCC 1331) and *V. cholerae* (ATCC 25837) in aqueous solution using the fixed bed mode of treatment of water. The breakthrough times for these composite adsorbents in the complete removal of 1.5×10^6 cfu/mL of these bacteria from solution is shown in Fig. 4(A–F). It is observed that PP-HYCA, PS-HYCA and PP-PS-HYCA composites have 400, 700, 275 min breakthrough times respectively for *S. typhi* removed from solution; and 400, 400, 200 min for *V. cholerae* removed from solution respectively (Fig. 4A–F). The result suggests that, for *S. typhi* and *V. cholera* removal from water, the combo composite (PP-PS-HYCA) showed the least efficiency while PS-HYCA composite showed the best efficiency. Both PP-HYCA and PS-HYCA composite adsorbents treated at least 3.2 L of water contaminated with 1.5×10^6 cfu/mL bacteria at a flowrate of 8 mL/min. However, for all three composite adsorbents used, they kept the levels of bacteria in solution far below alert/action levels of ca. 500 cfu/mL [55] even after ≥12 h of service time (Fig. 4A–F). This suggests that all three composites could be used for the removal of enteric gram-negative bacteria in water especially with PS-HYCA composite adsorbent which has the best efficiency.

We are of the opinion that the removal efficiency of these composites is a result of an interaction between the phosphate units on the cell walls of the bacteria and metal species on the surface of these composites. It has been suggested that these phosphate units from the bacteria cell walls form bonds with the metal oxide surface [56]. Given that the amount of Zn predominates over other metal present in the composites (Fig. 5A–C), it is logical to suggest that the metal responsible for bacteria capture in these composites is Zn (in the form of ZnO). Furthermore, there appears to be a correlation between the amount of Zn and the antibacterial activity of composite adsorbent (Fig. 5A–C). It is observed that the higher the amount of Zn in the composite, the better the antibacterial activity of the composite. However, with the presence of some other metals and non-metals, this activity appears to be compromised. This is consistent with breakthrough time data in Fig. 4 with PS-HYCA composite adsorbent showing the best efficiency in the capture these bacteria from aqueous solution (Fig. 5B, PS-HYCA composite adsorbent having the least interference from other metals and non-metals) and PP-PS-HYCA composite adsorbent showing the least efficiency in the capture these bacteria from aqueous solution (Fig. 5C, PP-PS-HYCA composite adsorbent having the most interference from other metals and non-metals).

Further experiments to confirm the efficiencies of PS-HYCA and PP-HYCA composite adsorbents in removing very low concentration of these bacteria from aqueous solution was carried out. With 10^3 cfu/mL of the bacteria in solution (a value slightly above the alert/action limits for bacteria in water), both PS-HYCA and PP-HYCA composite adsorbents kept the levels of *S. typhi* and *V. cholerae* in effluent solution at zero for up to 24 h.

To confirm the presence of a test bacterium on both PS-HYCA and PP-HYCA composite adsorbents (composites that were effective in the removal of these bacteria from water), the elemental mapping function in Scanning Electron Microscopy (SEM) technique was used to analyze bacteria-loaded composite adsorbents. The Back Scattered Electron (BSE) Detector was used. *Samonnella typhi*murium was selected as the test bacterium since the adsorbents were effective for the removal of this bacterium and also because SEM is primarily a qualitative technique. Thus, results obtained can be conveniently related to the adsorption of *V. cholerae* on these composite adsorbents. Confirmation for the adsorption of *E. coli* on these adsorbents was not considered because of the poor adsorption capacity of these composite adsorbents for the bacterium.

Fig. 6I and II show the elemental mapping images of *S. typhi*-loaded PS-HYCA and PP-HYCA composite adsorbents. It is observed that there is the presence of carbon in both composites evenly distributed on their surfaces which indicate the occurrence of dead pathogens (which are organic in nature and are majorly composed of carbon) on the surface of the composite adsorbents. A similar analysis carried out on the pristine composites indicated no observable presence of carbon on the surfaces of these composites (Figs. S1–S3). The presence of Zn in the composites further supports the successful doping of the metal into these adsorbents (Figs. S1–S3).

To further confirm the presence of the test bacteria on both PS-HYCA and PP-HYCA composite adsorbents, the Scanning Electron Microscopy technique was also used. Fig. 7I shows the SEM images of *S. typhi*-loaded composite adsorbents. Close examination of these images show that the surfaces of these composite particles are masked with small needle-like structures that are suggested to be the bacteria. This is further confirmed by the presence of carbon on these samples as earlier reported and shown in the elemental mapping images in Fig. 6IC and IIC.

Both elemental mapping analysis and SEM images support the fact that the removal mechanism of these enteric bacteria is by surface interaction and not via the pore of these composites since the pore sizes of PP-HYCA, PS-HYCA and PP-S-HYCA composites adsorbents are 2.82 nm, 3.20 nm and 3.07 nm respectively which are quite smaller than the sizes of any of these enteric bacteria which are in the micrometer range – ***S. typhi***: 0.7–1.5 μm by 2.0–5.0 μm [57]; and ***V. cholerae:*** 5–8 μm by 1.4–2.6 μm [58].

From this study and as earlier mentioned, it is understood that ZnO is the major site for interaction between the composite and the bacteria. ZnO could act either as a bactericidal or bacteriostatic agent [59]. In the former situation, ZnO neutralizes the bacterial surface potential resulting in electron-hole pair generation that enhances the production of reactive oxygen species (ROS) that inactivates and kill the bacteria [60]. However, in the latter form, as a bacteriostatic agent, it captures and subsequently inactivates the bacteria without killing them.

To confirm the mechanism by which the prepared composite adsorbents in this study removed these bacteria from aqueous solution; we carried out a simple viability test using sterile water, normal saline water and nutrient broth as described in Section 2.5.

It was observed that sterile water, which is expected to desorb loosely held bacteria (mostly by van der Waal forces) held on the composite adsorbent surfaces, showed some colonies of these bacteria as expected (Fig. 7II). However, with normal saline water (0.9% NaCl solution) and nutrient broth, colonies of bacteria would not be expected if the composite adsorbents operate the bactericidal mode. With the result shown in Fig. 9II (with lots of bacteria colonies in both saline water and nutrient broth samples), it implies that the composite adsorbents used in this study followed the bacteriostatic mode of removal of bacteria from aqueous solution rather than the bactericidal mode.

For the composite adsorbents prepared in this study to act as bacteriostatic agents, they must possess positive charges as an opposite charge to that of the gram-negative bacteria. Normally, ZnO is typically neutral when hydroxyls from water are attached to their surfaces [61]. In aqueous medium and at high pH, proton (H^+) on the hydroxyl is desorbed from the particle surface leaving a negatively charged surface with partially bonded oxygen atoms (ZnO^-). Conversely, at lower pH (below its isoelectric point of pH 9–10), protons from aqueous solution are transferred to the particle surface, leading to a positive charge ($ZnOH_2^+$) on the surface. In the case of our composite adsorbent, PP-HYCA, PS-HYCA and PS-PP-HYCA as shown in Fig. 8, their pH_{pzc} were found to be 7.0, 7.0 and 6.47 respectively. These values are below the isolectric point of ZnO.

This suggests that these composites will have positive charges below their pH_{pzc} and as such the surface charge of the composites should be positive [28,62]. Even at neutral pH of the aqueous solution, it has been established that the net charge of ZnO particles is positive [63].

In the course of studying the bacteria removal from aqueous solutions in this work, the pHs of influent solutions were measured and were found to be between 6.0 and 6.7 which are below the pH_{pzc} of the composite adsorbents. Apparently, it is expected that the surfaces of our composites will be positively charged, which explains the efficacy of these composites in the removal of gram-negative bacteria like *S. typhi* and *V. cholera* from aqueous solution. This bacteriostatic (electrostactic) effect has been confirmed by Leung and Co [64]. It is known that this electrostatic interaction can result in damaged molecular structure of phospholipids and consequently cell membrane damage [65,66]. However, their efficiencies now depend on the number of these positive charges on the surfaces. Thus, the more ZnO sites (which are the active sites) present on the composite, the better the efficacy of the composite as a bacteriostatic agent. On the other hand, the more the competing non-metal ion present on the surface of the composite, the less the bacteriostatic efficacy of the composite (Fig. 5) most likely because of competition for available active sites.

To confirm if Zn was leached into the treated water solution during the treatment process, several effluent samples were tested for Zn and Na ions using FAAS. It was observed that there were Zn ion and Na ion losses of ca. 0.46 mg/L and 0.20 mg/L respectively, into the treated water solution after 120 min of the adsorption process. These metal ions are from the bacteriostatic hybrid clay composite adsorbents which were prepared with $ZnCl_2$ and NaOH. These values are still far below World Health Organization (WHO) standard limit of 5 mg/L and 20 mg/L of Zn and Na in drinking water.

3.3. Regeneration

In this study, we attempted the regeneration of *S. typhi*-loaded adsorbents (as test samples) using the steam technique. A 1.5×10^6 cfu/mL of *S. typhi* bacteria was loaded on the composite adsorbents. Fig. 9 shows the results from the steam regeneration of *S-typhi* loaded PS-HYCA and PP-HYCA composite adsorbents respectively. With steam regeneration method, it was observed that the capacity of PS-HYCA composite adsorbent apparently decreased with subsequent regeneration such that after the 1st, 2nd, and 3rd regeneration cycles PS-HYCA composite adsorbent had a breakthrough time of 540 min (with 4.32 L of treated water produced), 540 min (4.32 L of treated water produced) and 480 min (3.84 L of treated water produced) respectively. However, PP-HYCA composite adsorbent gave a breakthrough time of 210 min (1.68 L of treated water produced), 180 min (1.44 L of treated water produced) and 180 min (1.44 L of treated water produced) respectively as shown in Fig. 9.

From the results, it is evident that PP-HYCA composite adsorbent lost 47.5%, 55% and 55% of its breakthrough time after the 1st, 2nd and 3rd regeneration cycles respectively while PS-HYCA composite adsorbent lost 22.9%, 22.9% and 31.4% of its breakthrough time after the 1st, 2nd and 3rd regenerations cycles respectively. The reduction in breakthrough time with increasing regeneration cycle is due to some loss in the adsorption capacity of the composite adsorbents which may be linked to loss of adsorbent weight owing to attrition.

These regeneration results suggest that the *Carica papaya* hybrid clay composite adsorbent (PS-HYCA) lost ca. 31% of its capacity after treating ca. 18 L for 1560 min of service time with three regenerations while plantain peel (*musa paradisiaca*) hybrid clay composite adsorbent (PP-HYCA) lost ca. 55% of its capacity after treating 4.56L for 570 min of service time with three regenerations. This supports our earlier findings in this study that the PS-HYCA composite adsorbent has better bacteriostatic efficiency, especially after the first two regeneration cycles.

With the observed loss in adsorption capacity of the adsorbent after 3 regeneration cycles, the PS-HYCA composite adsorbent was further heated in an oven @ 200 °C for 30 min after steam regeneration. The composite adsorbent was subsequently washed with sterilized distilled water and dried in an oven at 70 °C. The adsorption capacity, though not completely restored, was significantly improved over that which was steam regenerated, so that with the adsorption of *S. typhi* at a concentration of 1.5×10^6 cfu/mL, the breakthrough time of the composite adsorbent was at 600 min (Fig. 10). This suggests that for effective regeneration of the composite adsorbent, steam regeneration should accompany dry heating in an oven for a short period.

4. Conclusion

This preparation and characterization of agrogenic modified kaolinite doped with Zn in a microwave-assisted environment have been successfully achieved. Modification with *Carica papaya* seeds (PS-HYCA) produced a better composite adsorbent with better bacteriostatic efficiency for the removal of enteric bacteria (*S. typhi* and *V. cholerae*) from aqueous solution than plantain peel modified clay (PP-HYCA) composite adsorbent. A combination of both *Carica papaya* seeds and plantain peel was used in preparing the Hybrid clay composite adsorbent, PS-PP-HYCA. This composite adsorbent was not

as effective, in removal of bacteria (*S. typhi* and *V. cholerae*) from water, as either of the agrogenic biomasses used for the composite preparation. Results from Scanning Electron Microscopy, Electron Density Mapping and a simple viability test suggest that the mechanism for the removal of these bacteria from aqueous solution is by surface interaction via inactivation on the ZnO phase of the composites. Bacteria-loaded composite adsorbents were regenerated via steam regeneration technique and further heated in oven to renew the efficiency of *Carica papaya* prepared composite adsorbent for the removal of bacteria from aqueous solution. These composites, especially the *Carica papaya* prepared composite adsorbent, show promise for use in a point-of-use system for the efficient capture of gram-negative enteric bacteria from water.

Acknowledgements

The authors gratefully acknowledge funding from The World Academy of Sciences (TWAS) with a research grant (**10-215 RG/CHE/AF/AC_G-UNESCO FR: 324028613**) for this work. The support of the Redeemer's University, Nigeria, Department of Earth and Environmental Science, University of Potsdam, Potsdam, Germany and the Institute of Chemistry, Universität Potsdam, Germany is also highly appreciated.

Appendix A. Supplementary data

Supplementary data associated with this article can be found, in the online version, at http://dx.doi.org/10.1016/j.jece.2017.04.017.

References

[1] WHO, Drinking-Water, WHO Media Centre, 2015, http://www.who.int/mediacentre/factsheets/fs391/en/.
[2] O.F. Nwabor, E.I. Nnamonu, P.E. Martins, O.C. Ani, Water and waterborne diseases: a review, Int. J. Trop. Dis. Health 12 (2016) 1–14.
[3] O.A. Ayeni, A.S.O. Soneye, I.I. Balogun, State of water supply sources and sanitation in Nigeria: implications for muslims in Ikare-Akoko township, Arab World Geogr./Le Géographe du monde arabe 12 (2009) 95–104.
[4] J. Jadhav, K.S. Ravish, D. Gopinath, A study of socio-cultural factors, water quality and diarrhea In Bangalore, Internet J. Public Health 1 (2009) 1–5.
[5] J.V. Gagliardi, J.S. Karns, Leaching of Escherichia coli O157:H7 in diverse soils under various agricultural management practices, Appl. Environ. Microbiol. 66 (2000) 877–883.
[6] Z. Hong, X. Rong, P. Cai, K. Dai, W. Liang, W. Chen, Q. Huang, Initial adhesion of bacillus subtilis on soil minerals as related to their surface properties, Eur. J. Soil Sci. 63 (2012) 457–466.
[7] S.A. Bradford, V.L. Morales, W. Zhang, R.W. Harvey, A.I. Packman, A. Mohanram, C. Welty, Transport and fate of microbial pathogens in agricultural settings, Crit. Rev. Environ. Sci. Technol. 43 (2013) 775–893.
[8] C. Ferguson, A.M.R. Husman, N. Altavilla, D. Deere, N. Ashbolt, Fate and transport of surface water pathogens in watersheds, Crit. Rev. Environ. Sci. Technol. 33 (2013) 299–361.
[9] M.Q. Xue, J. Li, Z.M. Xu, Environmental friendly crush-magnetic separation technology for recycling metal-plated plastics from end-of-life vehicles, Environ. Sci. Technol. 46 (2012) 2661–2667.
[10] M. Zhang, B. Gao, S. Varnoosfaderani, A. Hebard, Y. Yao, M. Inyang, Preparation and characterization of a novel magnetic biochar for arsenic remova, Bioresour. Technol. 130 (2013) 457–462.
[11] H. Ma, B. Hsiao, B. Chu, Functionalized Electrospun Nanofibrous microfiltration membranes for removal of bacteria and viruses, J. Membr. Sci. 452 (2014) 446–452.
[12] R.D. Ambashta, M. Sillanpaa, Water purification using magnetic assistance: a review, J. Hazard. Mater. 180 (2010) 38–49.
[13] X. Nie, G. Li, M. Gao, H. Sun, X. Liu, H. Zhao, P.K. Wong, T. An, Comparative studyon the photo-electrocatalytic inactivation of Escherichia coli K-12 and its mutant Escherichia coli BW25113 using TiO2nanotubes as a photoanode, Appl.Catal. B: Environ. 147 (2014) 562–570.
[14] V.K. Agrawal, R. Bhalwar, Household water purification: low-cost interventions, MJAFI 65 (2009) 260–263.
[15] M. Amin, A. Alazba, U. Manzoor, A review of removal of pollutants from water/wastewater using different types of nanomaterials, Adv. Mater. Sci. Eng. (2014), http://dx.doi.org/10.1155/2014/825910.
[16] T. Karanfil, B. Mitch, P. Westerhoff, Recent advances in disinfection by-products, vibrational spectroscopy and other novel techniques, ACS Symposium Series, Ameican Chemical Society, Washington, DC, 2015.
[17] Q. Li, S. Mahendra, D.Y. Lyon, L. Brunet, M.V. Liga, D. Li, P.J. Alvarez, Antimicrobial nanomaterials for water disinfection and microbial control: potential applications and implications, Water Res. 42 (2008) 4591–4602.
[18] R. Nassar, E. Browne, J. Chen, A. Klibanov, Removing human immune deficiency-virus (HIV) from human blood using immobilized heparin, Biotechnol. Lett. 34 (2012) 853–856.
[19] K. Pankaj, R. Tyagi, V. Smriti, K. Dharmendra, T. Shruti, Nanomaterials use in wastewater treatment, International Conference on Nanotechnology and Chemical Engineering (ICNCS'2012), Bangkok, Thailand, 2012.
[20] N. Savage, M.S. Diallo, Nanomaterials and water purification: opportunities and challenges, J. Nanopart. Res. 7 (2005) 331–342.
[21] H. Zhang, Application of Silvernanoparticles in Drinking Water Purification, Civil and Environmental Engineering, University of Rhode Island, USA, 2013.
[22] G. Ghasemzadeh, M. Momenpour, F. Omidi, M.R. Hosseini, M. Ahani, A. Barzegari, Applications of nanomaterials in water treatment and environmental remediation, Front. Environ. Sci. Eng. 8 (2014) 471–482.
[23] M.C. Stensberg, Q. Wei, E.S. McLamore, D.M. Porterfield, A. Wei, S. Sepulveda, Toxicological studies on silver nanoparticles: challenges and opportunities in assessment, monitoring and imaging, Nanomedicine 6 (2011) 879–898.
[24] L. Fewtrell, Silver: Water Disinfection and Toxicity Centre For Research into Environment and Health, (2014), pp. 1–53, www.who.int/water_sanitation_health/dwq/chemicals/Silver_water_disinfection_toxicity_2014v2. pdf.
[25] E.I. Unuabonah, A. Taubert, Clay–polymer nanocomposites (CPNs): adsorbents of the future for water treatment, Appl. Clay Sci. 99 (2014) 83–92.
[26] E.I. Unuabonah, C. Gunter, J. Weber, S. Lubahn, A. Taubert, Hybrid clay: a new highly efficient adsorbent for water treatment, ACS Sustain. Chem. Eng. 1 (2013) 966–973.
[27] K.O. Adebowale, E.I. Unuabonah, B.I. Olu-Owolabi, Adsorption of some heavy metal ions on sulfate- and phosphate modified Kaolin, Appl. Clay Sci. 29 (2005) 145–148.
[28] D. Dayananda, V.R. Sarva, S.V. Prasad, J. Arunachalam, P. Parameswaran, N.N. Ghosh, Synthesis of MgO nanoparticle loaded mesoporous Al2O3 and its defluoridation study, Appl. Surf. Sci. 329 (2015) 1–10.
[29] S. Polarz, B. Smarsly, Nanoporous materials, J. Nanosci. Nanotechnol. 2 (2002) 581–612.
[30] J. Yang, K. Qiu, Preparation of activated carbon from walnut shell via vacuum chemical activation and their application for methylene blue removal, Chem. Eng. J. 165 (2010) 209–217.
[31] J. Kong, S. Yu, Fourier transform infrared spectroscopic analysis of protein secondary structures, Acta Biochim. Biophys. Sin. 39 (2007) 549–559.
[32] E.I. Unuabonah, K.O. Adebowale, B.I. Olu-Owolabi, Kinetic and Thermodynamic studies of the adsorption of lead (II) ions onto phosphate-modified Kaolinite clay, J. Hazard. Mater. 144 (2007) 386–395.
[33] N. Worasith, B.A. Goodman, N.J. Paitip, Decolorization of rice bran oil using modified kaolin, J. Chem. Soc. Oil 88 (2014) 2005–2014.
[34] D.M. Moore, R.C. Reynolds Jr., X-ray Diffraction and the Identification and Analysis of Clay Minerals, Oxford University Press, New York, 1989.
[35] M. Guessoum, S. Nekkaa, F. Fenouillot-Rimlinger, N. Haddaoui, Effects of kaolin surface treatments on the thermomechanical properties and on the degradation of polypropylene, J. Polym. Sci. (2012), http://dx.doi.org/10.1155/2012/549154.
[36] S. Attia, N. Chaari, S. Chaabouni, Synthesis, crystal structure, and dielectric properties of (3-aminopropyl-imidazolium) pentachlorobismuthate (III) $[C_6H_{13}N_3]BiCl_5$, J. Cluster Sci. 26 (2015) 1343–1359.
[37] B. Stuart, Infrared Spectroscopy: Fundamentals and Applications, John Wiley & Sons Ltd, Chichester, 2004.
[38] H. Barrak, T. Saied, P. Chevallier, G. Laroche, A. M'nif, A.H. Hamzoui, Synthesis, characterization, and functionalization of ZnO nanoparticles by N-(trimethoxysilylpropyl) ethylenediamine triacetic acid (TMSEDTA): Investigation of the interactions between Phloroglucinol and ZnO@TMSEDTA, Arab. J. Chem. (2016), http://dx.doi.org/10.1016/j.arabjc.2016.04.019.
[39] J. Han, H. Su, J. Xu, W. Song, Y. Gu, Y. Chen, W.-J. Moon, D. Zhang, Silk-mediated synthesis and modification of photoluminescent ZnO nanoparticles, J. Nanopart.Res. 14 (2012) 726.
[40] A.E. Raevskaya, O.L. Stroyuk, D.L. Solonenko, V.M. Dzhagan, D. Lehmann, S. YaKuchmiy, V.F. Plyusnin, D.R.T. Zahn, Synthesis and luminescent properties of ultrasmall colloidal CdS nanoparticles stabilized by Cd(II) complexes with ammonia and mercaptoacetate, J. Nanopart. Res. 16 (2014) 2650.
[41] B. Nandi, R. Uppalu, M. Purkait, Preparation and characterization of low cost ceramics membranes for microfiltration applications, Appl. Clay Sci. 42 (2008) 102–110.
[42] N. Salahudeen, A.S. Ahmed, A.H. Al-Muhtaseb, M. Dauda, S.M. Waziri, B.Y. Jibril, Synthesis and characterization of micro-sized silica from kankara kaolin, J. Eng. Res. 19 (2014) 27–32.
[43] A. Taubert, G. Glasser, D. Palms, Kinetics and particle formation mechanism of zinc oxide particles in polymer-controlled precipitation from aqueous solution, Langmuir 18 (2002) 4488–4494.
[44] Z. Li, A. Shkilnyy, A. Taubert, Room temperature ZnO mesocrystal formation in the hydrated ionic liquid precursor (ILP) tetrabutylammonium hydroxide, Cryst. Growth Des. 8 (2008) 4526–4532.
[45] D.M. Moore, R.C. Reynolds Jr., X-ray Diffraction and the Identification and Analysis of Clay Minerals, Oxford University Press, New York, 1997.
[46] S. Talam, S.R. Karumuri, N. Gunnam, Synthesis, characterization, spectroscopic properties of ZnO nanoparticles, ISRN Nanotechnol. (2012), http://dx.doi.org/10.5402/2012/372505.
[47] M.R. Khanlary, V. Vahedi, A. Reyhani, Synthesis and characterization of ZnO nanowires by thermal oxidation of Zn films at various temperatures, Molecules 17 (2012) 5021–5029.
[48] D.P. Serrano, R.V. Grieken, M.E. Davis, J.A. Melero, A. Gracia, G. Morales,

Mechanism of CIT-6 and VPI-8 crystallization from zincosilicate gels, Chem. Eur. J. 8 (2002) 5153–5160.
[49] M.M.J. Treacy, J.B. Higgins, Collection of Simulated XRD Powder Patterns for Zeolites, Elsevier, Amsterdam – London – New York – Oxford – Paris – Shannon – Tokyo, 2001pp. 586.
[50] M. Gusatti, C.E.M. Campos, J.A. Rosário, D.A.R. Souza, N.C. Kuhnen, H.G. Riella, The rapid preparation of ZnO nanorods via low-temperatures solochemical method, J. Nanosci. Nanotechnol. 11 (2011) 5187–5192.
[51] D.O. Okorie, C.O. Eleazu, P. Nwosu, Nutrient and heavy metal composition of plantain (Musa paradisiaca) and banana (Musa paradisiaca) peels, J. Nutr. Food Sci. 5 (2015) 370–372.
[52] E.K. Marfo, O.L. Oke, O.A. Afolabi, Chemical composition of papaya (Carica papaya) seeds, Food Chem. 22 (1986) 259–266.
[53] G. Aravind, D. Bhowmik, S. Duraivel, G. Harish, Traditional and medicinal uses of carica papaya, J. Med. Plants Stud. 1 (2013) 7–15.
[54] J.K. Peter, Y. Kumar, P. Pandey, H. Masih, Antibacterial activity of seed and leaf extract of carica papaya var. pusa dwarf linn IOSR, J. Pharm. Biol. Sci. 9 (2014) 29–37.
[55] V.T.C. Penna, S.A.M. Martins, P.G. Mazzola, Indentification of bacteria in Drinlking and purified water during the monitoring of a typical water purification system, BMC Public Health 2 (2002) 13.
[56] P.H. Mutin, G. Guerrero, A. Vioux, Hybrid materials from organo-phosphorus coupling molecules, J. Mater. Chem. 15 (2005) 3761–3768.
[57] S.G.B. Huehn, Development and Validation of a DNA Microarray for Characterisation and Typing of Salmonella Isolates, Fachbereich Biologie, Chemie, Pharmazie der Freien Universität zu Berlin, Berlin, 2009.
[58] G. Diuret, A.H. Delcour, Sizes and dynamics of Vibrio cholerae porins OmpT and OmpT by polmer exclusio, Biophys. J. 98 (2010) 1820–1829.
[59] Y. Xie, Y. He, P.L. Irwin, T. Jin, X. Shi, Antibacterial activity and, mechanism of action of zinc oxide nanoparticles against *Campylobacter jejuni*, Appl. Environ. Microbiol. 77 (2011) 2325–2331.
[60] M. Arakha, M. Saleem, B.C. Mallick, S. Jha, The effects of interfacial potential on antimicrobial propensity of ZnO nanoparticle, Sci. Rep. 5 (2015), http://dx.doi.org/10.1038/srep09578.
[61] F. Qu, P.C. Morais, The pH dependence of the surface charge density in oxide-based semiconductor nanoparticles immersed in aqueous solution, IEEE Trans. Magn. 37 (2001) 2654–2666.
[62] J. Rivera-Utrilla, I. Bautista-Toledo, M.A. Ferro-Garcia, C. Moreno-Castilla, Activated carbon surface modifications by adsorption of bacteria and their effect on aqueous lead adsorption, J. Chem. Technol. Biotechnol. 76 (2001) 1209–1215.
[63] M. Baek, M.K. Kim, H.J. Cho, J.A. Lee, J. Yu, H.E. Chung, S.J. Choi, Factors influencing the cytotoxicity of zinc oxide nanoparticles: particle size and surface charge, J. Phys.: Conf. Ser. 304 (2011), http://dx.doi.org/10.1088/1742-6596/1304/1081/012044.
[64] Y.H. Leung, X. Xu, A.P.Y. Ma, F. Liu, A.M.C. Ng, H.K. Lee, W.K. Chan, F.C.C. Leung, Toxicity of ZnO and TiO_2 to Escherichia coli cells, Sci. Rep. 6 (2016) 35243, http://dx.doi.org/10.1038/srep35243.
[65] W. Jiang, K. Yang, R.W. Vachet, B. Xing, Interaction between oxide nanoparticles and biomolecules of the bacterial cell envelope as examined by infrared spectroscopy, Langmuir 26 (2010) 18071–18077.
[66] K. Rajavel, R. Gomathi, S. Manian, R.T. Rajendra Kumar, In vitro bacterial cytotoxicity of CNTs: reactive oxygen species mediate cell damage edges over direct physical puncturing, Langmuir 30 (2013) 592–601.